

Review Article

Infrared–Resin Crack Measurement and Preventive Work Technology for Maintenance

Nobuhiro Shimoi^{1,*} , Yu Yamauchi¹ , Kazuhisa Nakasho² 

¹Faculty of Systems Science and Technology, Akita Prefectural University, Yurihonjo, Japan

²Graduate School of Sciences & Technology for Innovation, Yamaguchi University, Ube, Japan

Abstract

The use of thermography as a nondestructive evaluation technique is increasingly popular for maintaining concrete structures. Most inspections merely evaluate the locations and shapes of defects on surfaces. To address this shortcoming, it proposes an inspection method and preventive work using a coating-type resin sensor combined with an infrared camera. No method has been developed to assess the depth of defects. In this approach, infrared-reactive resin is applied. Thermographic images of the target area are captured sequentially. Temperature curves obtained at each pixel during the cooling process are analyzed using Fourier transform to differentiate defect states in various parts of the temperature distribution. The temperature change is found to be correlated with the defect size. Approximately 5% aluminum powder is mixed into the applied gel resin. Because of its specific gravity, it tends to concentrate in areas damaged by compression failure or to float. This report discusses technologies related to identification of defects and measuring their size in infrared-reactive resin, with examination of the effectiveness of measures to prevent scattering and collapse of defects caused by structural degradation. A concentric loading test on reinforced concrete columns confined by gel resin ties is described herein. Test variables include concrete compressive strength of 232–244 N/mm², both below and above the equipment hole that caused the defect, and to measure the relation, a comparison with test specimens that are free of defects.

Keywords

Health Monitoring, Infrared Thermography, Non-Destructive Inspection, Reinforcement, Spalling Prediction

1. Introduction

Long-term, constant monitoring of deterioration and structural changes is important because such changes strongly affect social safety and security. The realization of such monitoring can be supported by measurement and evaluation methods after fully elucidating aspects of the usage environment, such as the characteristics of the structure to be measured and its duration of use. The development of

new monitoring technologies is therefore urgently necessary [1]. To realize such monitoring of structural integrity, one must fully understand the characteristics of the structure to be measured and the usage environment, such as the number of years of use. Then one can consider measurement and evaluation methods before implementing them. Maintaining the soundness of infrastructure reliably requires accurate

*Corresponding author: Shimoi@Akita-pu.ac.jp (Nobuhiro Shimoi)

Received: 24 April 2024; **Accepted:** 16 May 2024; **Published:** 3 June 2024



Copyright: © The Author(s), 2024. Published by Science Publishing Group. This is an **Open Access** article, distributed under the terms of the Creative Commons Attribution 4.0 License (<http://creativecommons.org/licenses/by/4.0/>), which permits unrestricted use, distribution and reproduction in any medium, provided the original work is properly cited.

evaluation of the state of structures by judging the presence, frequency, and location of damage based on survey and inspection data. Specifically, we quantify empirical evaluation methods such as “visual inspection” and “hammering inspection.” Further improvement of the efficiency of “nondestructive inspections” such as X-ray inspection and magnetic flaw detection (standardization, cost reduction, etc.) and high performance (improvement of accuracy, automatic data judgment, etc.) are important [2]. Therefore, the authors have developed a method to measure the soundness of concrete piers of bridges, inner walls of tunnels, and tiled walls of high-rise buildings in a simple, long-term, inexpensive manner. The method is useful to identify anomalies such as concrete cracks, defects, and wall floats. The technical method was examined. Our findings suggest that certain difficulties can be resolved using the original infrared reactive resin and image analysis technology that enables passive measurement using a long-wave infrared camera. This technology is based mainly on active measurement such as heating and pre-cooling because of temperature changes of the measurement object, which are usually measured using an infrared camera. To enable passive measurement at room temperature (20 °C), we devised the idea of mixing aluminum powder into the gel resin [2]. Then we applied it to the concrete to be treated. If done when a crack occurs on the concrete wall surface shown in Figure 1(a) or when a float and crack shown in Figure 1(b) occurs, then the aluminum powder in the gel resin flows and concentrates at the defect. Therefore, after the wall retains heat from sunlight, the missing part is highlighted by the temperature difference between the infrared radiation and the atmosphere. Furthermore, even if no heat radiation from sunlight is incident on the wall surface, then detecting defects and anomalies from the temperature difference between the wall surfaces is possible because of differences in materials: the aluminum powder in the gel resin creates a radiative cooling effect [2-4]. That effect can be read as a representative signature. The coated gel resin for this measurement also has a repair effect: it flows into cracks and defects because of differences in specific gravity between the resin and metal. Therefore, this measurement method can be regarded as a measurement technology serving both as a measure of defects in concrete walls and as a preventive measure. Reportedly, rainwater flowing into the concrete structure from a defective area flows into gaps and causes rain leakage, thereby accelerating deterioration [5]. To verify our proposed technology, nine concrete test specimens were created and tested under different conditions. This report presents results of verification of crack progression characteristics and measurement effects assessed through destructive testing. In recent years, a method has been applied of using a visible light camera to measure “lifting” and “surface cracking” related to corrosion of concrete reinforcement. Unfortunately, visible light cameras are limited to measurement of the surface only. By contrast, infrared cameras can measure conditions deep under the surface [2].

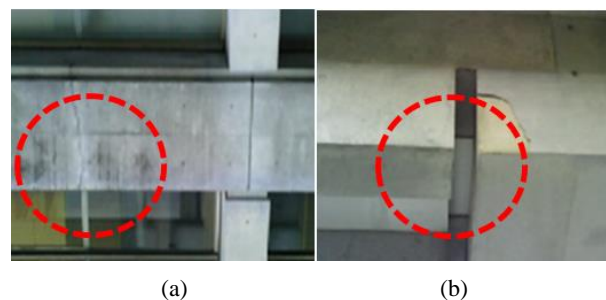


Figure 1. Concrete peeling and occurrence situation on a concrete surface, in images taken using a visible light camera.

2. Gel-Type Coating Resin for Sensor

In recent years, external cameras have been used to measure “float” and “surface cracks” related to reinforcing steel corrosion in concrete. However, when an infrared camera is used, the resolution is 1920×1200 pixels in the 8–14 μm infrared wavelength band; it is only 640×512 pixels in the 3–5 μm infrared wavelength band. In other words, there is a reason why it is necessary to narrow down the detection locations. Also, the radiant energy of infrared rays is proportional to the temperature. An infrared camera detects infrared energy and converts it into a pseudo-temperature image. The detection wavelength of infrared rays is probably around the middle infrared wavelength. The radiant energy of infrared rays is proportional to the temperature.

The heat energy density is expected to increase as it decreases. But the infrared camera detection wavelength of infrared rays is probably around the middle infrared wavelength. It is expected that the density of heat energy will increase as it decreases.

2.1. Consideration of Conventional Technology

Various methods are used for the quantitative evaluation of structural soundness for purposes of disaster prevention and mitigation. As sensor systems for measuring displacement and vibration because of static load, several methods can be used: measuring displacement using a laser displacement meter or a contact-type displacement meter, measuring natural vibration with a micro-vibration meter, and analyzing the fracture state and stress concentration using finite element method (FEM) analyses. There are also methods to identify locations [6]. In addition, X-ray analysis using FEM is useful as a non-destructive and quantitative method for evaluating residual stress in structures, but it is difficult to analyze crack growth using this method. Among these methods, micro-tremor vibration measurement yields the Fourier spectrum ratio of vertical and horizontal motion components, normalizes the horizontal vibration to the vertical vibration, and determines the amplification characteristics and natural period of the structure. The measurement system comprises a microtremor meter, a data logger, and a PC. Other methods

can also obtain those results [2]. The laser Doppler velocimeter (LDV) method [7] detects the velocity from the phase difference attributable to the Doppler effect between the irradiated light and the reflected light when the object is irradiated with laser light. This measurement system, which consists of two LDV devices, a data logger, a PC, and a digital displacement gauge, costs about 4.5–6 million yen per measurement unit. In addition, X-ray non-destructive equipment can be installed for monitoring limited areas, but it is not practical for long-term measurements because it requires equipment costs of about 8–10 million yen. Moreover, it requires a power supply [2]. By contrast, the thermographic wall inspection technology of structures using an infrared camera assesses temperature differences caused by sunlight insulating the outer wall of the building. Then it evaluates differences in wall material conductivity to measure differences that occur in the defective part. Variations arise depending on the crack size, depth, and condition [8]. We have developed a technique for image filter processing methods that emphasizes damaged areas shown in an infrared thermal image. Moreover, we are devising a statistical method for probabilistic prediction of damage as an index of the degree of damage according to temperature differences [9]. They are methods of extracting a defective area from an image based on the feature amount of a processed image. Nakamura et al. of Kyoto University used infrared thermography to measure specimens at each damage stage in a reinforcement corrosion expansion pressure simulation test for quantitative evaluation of spalling risk [2]. The degree of spalling risk is calculated as an index that can evaluate the degree of deterioration without considering the form [9–11]. To evaluate the safety and soundness of concrete structures, long-term monitoring of more than 20 years is considered necessary. However, a problem exists that a measuring device able to guarantee the required monitoring period and a smart sensing method that enables danger prediction have never been reported [12–14].



Figure 2. IR Camera.

In recent years, Hashizume et al. of Western Japan Expressway Engineering have achieved good results using a developed device, the J System, which can detect damage up to 4 cm height using infrared rays in the 3–5 μm band. The J System price is approximately 20 million yen (approx. US \$133,000) [15]. Table 1 presents specifications of the infrared camera used for measurement. Figure 2 presents a drawing of the camera used for the test [15].

Table 1. Infrared camera specifications.

Model	InfRec R450; Nippon Avionics Co., Ltd.
Detector	Two-dimensional non-cooling method
Measurement temperature range	-40 to 1500 $^{\circ}\text{C}$
Measurement wavelength	8 to 14 μm
Number of pixels	480 \times 360
Measurement field of view	24 deg \times 18 deg
Standard lens	10 cm to ∞
Weight	3.8 kg

2.2. Issues Related to Structure Monitoring

Objects that exist at room temperature emit energy by infrared radiation. Planck's law of radiation, expressed in equation (1), states that an object emits energy proportional to the fourth power of its absolute temperature. Boltzmann's law is presented in equation (2) hereinafter [16].

$$E(\lambda T) = \frac{2hc^2}{\lambda^5} \frac{1}{e^{hc/\lambda KT} - 1} [W/(m^2\mu m)] \quad (1)$$

$W\lambda b$: Black body spectral radiant emittance at wavelength λ

c : Speed of light 3×10^8 [m/s]

h : Planck's constant (6.6×10^{-27} Js)

K : Boltzmann's constant (1.38×10^{-16} J/K)

T : Absolute blackbody temperature (K)

λ : Wavelength (m)

$$t^4 [W / m^2] \quad (2)$$

Wb : Integrating the wavelength from $\lambda = 0$ to $\lambda = \infty$ from Planck's formula

Black body spectral radiance $-8.2 (W \cdot SR^{-1} \cdot m^2)$

σ : Boltzmann's constant (5.7×10^{-8} W/m 2)

t : Absolute blackbody temperature (K)

$$\lambda_{\max} = 2897/T [\mu m] \quad (3)$$

When the measurement target is 40 $^{\circ}\text{C}$ (absolute temperature $T = 273 + 40 = 313$ K), wavelength λ is $2897 \div 313 =$ approximately 9.2 μm from equation (3).

3. Reinforced Concrete Test Specimen and Measurement Method

Figure 3 presents the measurement status of a compressive fracture test of a reinforced concrete specimen using a force testing machine (5000 kN maximum force). For the destruc-

tive test, a maximum force of approximately 2200 kN was gradually applied vertically from the top of the specimen using a force testing machine. The specimen was destroyed completely after approximately 20 min. Figure 5 shows the steel frame of the reinforced concrete test specimen ($300 \times 400 \times 1000$ mm). The test specimen was produced using ordinary concrete with cover thickness of approx. 20 mm. To measure the effect on the test specimen strength, a through hole with 65 mm diameter was created artificially in specimens B and C to simulate defects in the concrete pillars. The through hole for specimen B was placed to the left of the central reinforcing bar 300 mm below the top of the specimen, and for specimen C to the left of the central reinforcing bar 700 mm below the top of the specimen. Furthermore, to evaluate the measurement effect of the infrared camera and the effectiveness of the use of gel resin as a sensor for preventing damage, we added approximately 0.2 mm to the front, back, left side, and right side of the specimen. The thickness of the gel resin (CY52-276; Dow Toray Co. Ltd.) was applied and compared with a test piece to which nothing was applied. To evaluate the gel-like resin properties, we used aluminum powder to prepare an aluminum-containing gel-like resin mixed. The aluminum-containing gel-like resin is made by adding micrometer-order aluminum powder to the gel-like resin at a concentration of 5 w/w % and stirring it well [2]. The gel-like resin used in this experiment is resistant to ultraviolet rays and is easy to handle because the coating does not harden over time. When in use, parts 1 and 2 are mixed in equal parts. They harden in about 1 hour. The resin has gel-like properties by which it adheres to the surface. Figure 3 presents a structural drawing of the compressive loading machine and the specimen ($300 \times 400 \times 1000$ mm) used for the 500 t compression test.

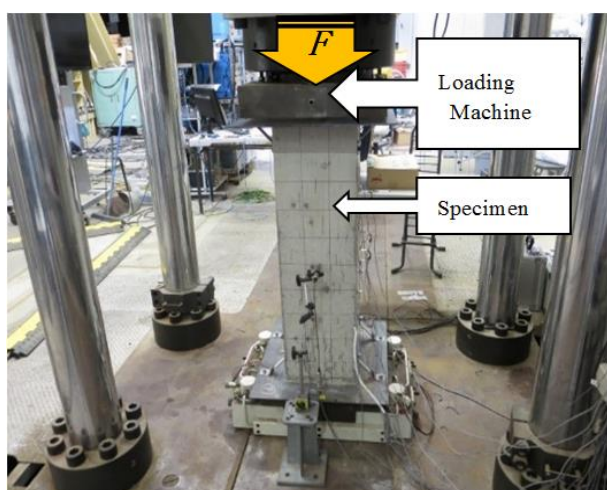


Figure 3. Structural drawing of the compressive loading machine and the specimen ($300 \times 400 \times 1000$ mm) used for the 500 t compression test.

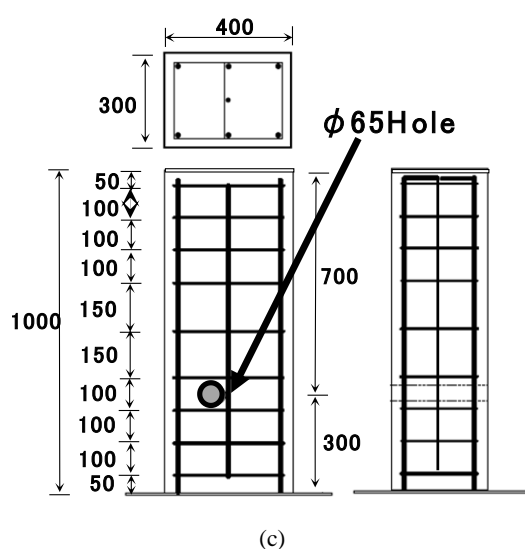
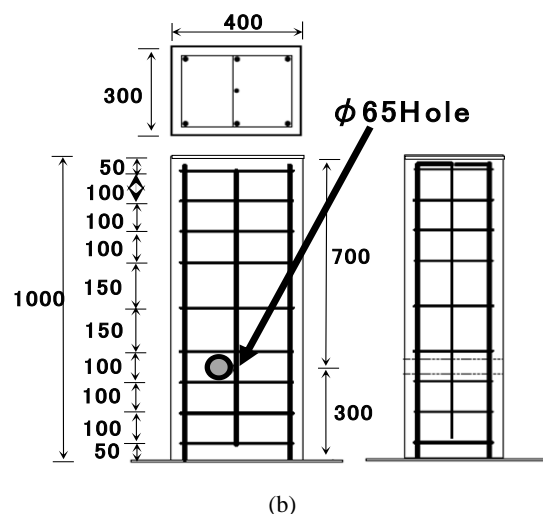
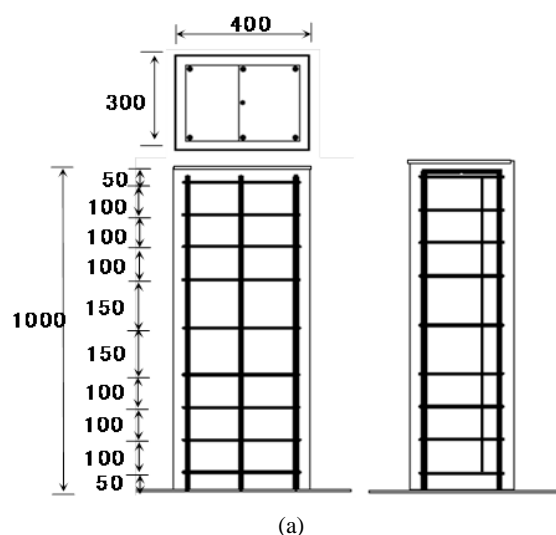


Figure 4. Experiment using equipment and specimens. (unit: mm).

4. Measurement Considerations and Results

4.1. Measurement of Surface Deformation Using an Infrared Reactive Coated Resin Sensor and Evaluation of Results

Destructive tests were conducted using reinforced concrete specimens A, B, and C as shown in Figure 5. No pretreatment such as residual heat was performed during destructive

testing. To verify the gel-like resin effects on test specimens of various shapes, we prepared the following: (i) some specimens had nothing coated on the sides; (ii) some specimens had gel-like resin (no mixture) coated onto four sides; (iii) some specimens had gel-like resin containing 5% aluminum coated on the four side surfaces. The total test specimens included nine types for comparison. Figure 5 presents visible light and infrared images of specimens after maximum loading. Cracks and floats were generated in the test specimens because of the compressive force applied from the top. These were measured using infrared thermal imaging.

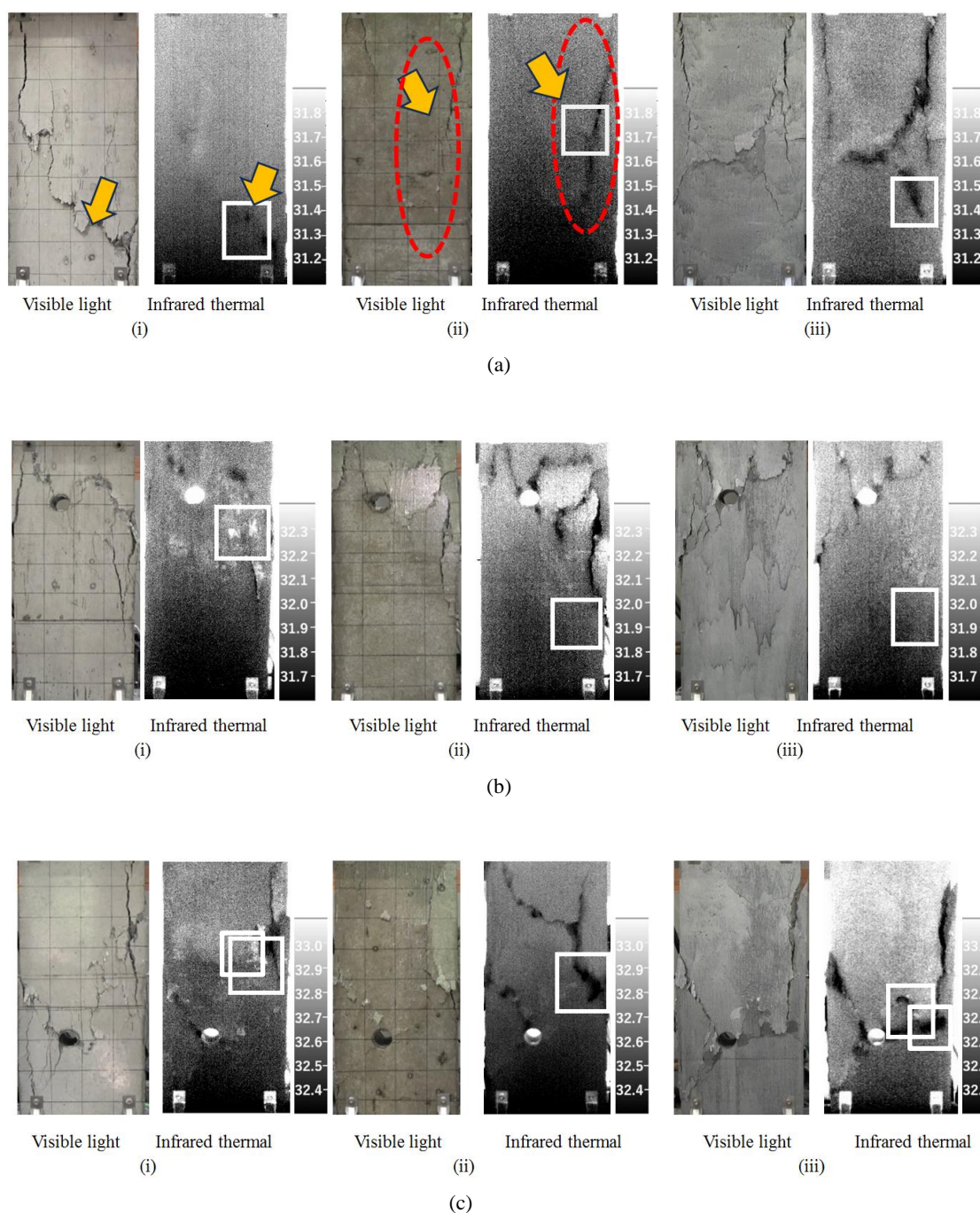


Figure 5. Comparison of visible light and infrared images with and without resin coating of specimens A, B, and C generated in the test specimens because of the compressive force applied from the top. These were measured using infrared thermal imaging.

Destructive test results for healthy specimen A are presented in Figure 5(a). Images taken with a visible light camera of the test specimen without the gel resin applied in (i) showed large bulges because of damage caused by the load applied from the top of the test specimen, and because of extensive surface peeling. Concrete pieces were scattered and collapsed because of shear force and compressive failure occurring diagonally downward from the upper right corner. Infrared images of the same test specimen also showed cracks that were difficult to measure from visible light images. Moreover, in the visible light image of specimen A coated with (ii) gel-like resin (no mixture), the crack that formed from the top of the specimen toward the center appeared to stop midway; it did not extend to the bottom. It will be done. Visual inspection shows an apparent bulge in the area indicated by the arrow in the visible light image, but this bulge could not be confirmed from the image. By contrast, an infrared thermal image of the same test piece shows that the crack which started at the top of the test piece extended to the bottom, and also extended considerably to the bulge area shown by the arrow, forming a deep crack. In the visible light image of specimen A coated with gel-like resin containing 5% aluminum in (iii), the cracks extension was slight, with a little peeling on the specimen surface. The appearance of cracks strongly suggests a preventive effect of the gel-like resin. In addition, the infrared thermal image of the same test piece realistically depicts the heat retention effect of the aluminum powder mixed with the gel-like resin that has penetrated into the crack, showing the state of the crack. Figure 5(b) presents destructive test results for specimen B, for which a defect was created in the upper part of the specimen. From a visible light camera image of the test specimen (i) without gel resin applied, it is possible to determine the state in which a crack has occurred, centered on the $\phi 65$ hole at the top. Furthermore, the infrared thermal image of the same test piece shows the peeling state on the test piece surface, visualized in white. From the visible light camera image of specimen B coated with gel-like resin (no mixture) in (ii), the surface peeling appears to be less than that of specimen (i). The infrared thermal image of the same specimen shows the crack size and depth, which were difficult to ascertain from visible light images. In the visible light camera image of specimen B coated with gel-like resin containing 5% aluminum in (iii), the crack propagation is less than that in (i) or (ii): even deep cracks appear to be gel-like. This finding seems to indicate effectiveness of the damage prevention effect of the resin. The infrared thermal image of the same test piece seems to show that the crack formation is limited to the vicinity of the hole, and that the progress of crack propagation to the surrounding area is slow. Figure 5(c) presents destructive test results for specimen C, in which a defect was created below the specimen. From the visible light camera image of specimen C without gel resin applied in (i), it can be found that a crack has occurred centered around the $\phi 65$ defect at the bottom. An infrared thermal image of the same test piece re-

vealed the peeling area well, making it possible to make a judgment. A visible light image of specimen C coated with the gel-like resin (no mixture) in (ii) shows fewer cracks and less surface peeling than in (i). In contrast to the visible light image, the infrared thermal image of this specimen visualizes damage in hidden parts that are difficult to detect with visible light. Furthermore, in the visible light camera image of specimen C coated with gel-like resin containing 5% aluminum in (iii), cracks are generally visible around the hole at the bottom and on the right side of the top. An infrared thermal image of the same test specimen depicts bulges caused by floating occurring from the top. Also, deep cracks have formed around the holes at the bottom.

These results prove the capability of using infrared thermal images to measure cracks and invisible areas of cracks that are difficult to detect from visible light images. This gel resin applied to the test piece surface exerts a heat-insulating effect, maintaining a difference between the test piece surface temperature and the room temperature. As a result of this capability of obtaining temperature measurements according to the theoretical formula for infrared thermal imaging, clear infrared thermal images can be obtained and used for analyses. Visualization using images has been achieved [17]. Furthermore, the gel-like resin appears to be effective as a preventive measure: it prevents cracks progression and prevents test specimen destruction by applied force.

4.2. Results of Crack Occurrence and Surface Temperature Changes over Time

We evaluated temperature changes on the surfaces of specimens A, B, and C during destructive tests when cracks occurred. For the respective specimens, (i) no coating was applied, (ii) gel-like resin (no mixture) was coated onto four side surfaces, and (iii) gel-like resin containing 5% aluminum was coated onto four surfaces. Thereby, results for nine objects of three types were compared. Figure 6 shows the time-series temperature changes of a crack that was determined to have the greatest temperature change in infrared thermal imaging measurements among the cracks that occurred in each test specimen. The value represents the difference between the maximum and minimum temperatures measured within a 100 mm square white line frame in the infrared image of each test specimen in Figure 6. The temperature was acquired at 20 Hz. Then the temperature difference over 5 s was calculated using a moving average. It represents the numerical value. In addition, to present the timing at which cracks occurred, the applied force value (2200 kN maximum load) measured simultaneously is also displayed in Figure 6. Figure 6(a) portrays a healthy test specimen A with no defects. Figure 6(b) exhibits a test specimen B with a $\phi 65$ hole created as a defect in the upper part of the specimen. Figure 6(c) depicts a $\phi 65$ hole in the lower part of the specimen. These are the results for test

specimen C with holes made. For each test specimen, (i) represents a specimen without gel resin applied, (ii) denotes a specimen with gel resin (no mixture) applied on four surfaces, and (iii) represents a specimen with four surfaces coated with gel resin (no mixture). A test specimen coated with 5% aluminum gel-like resin is shown.

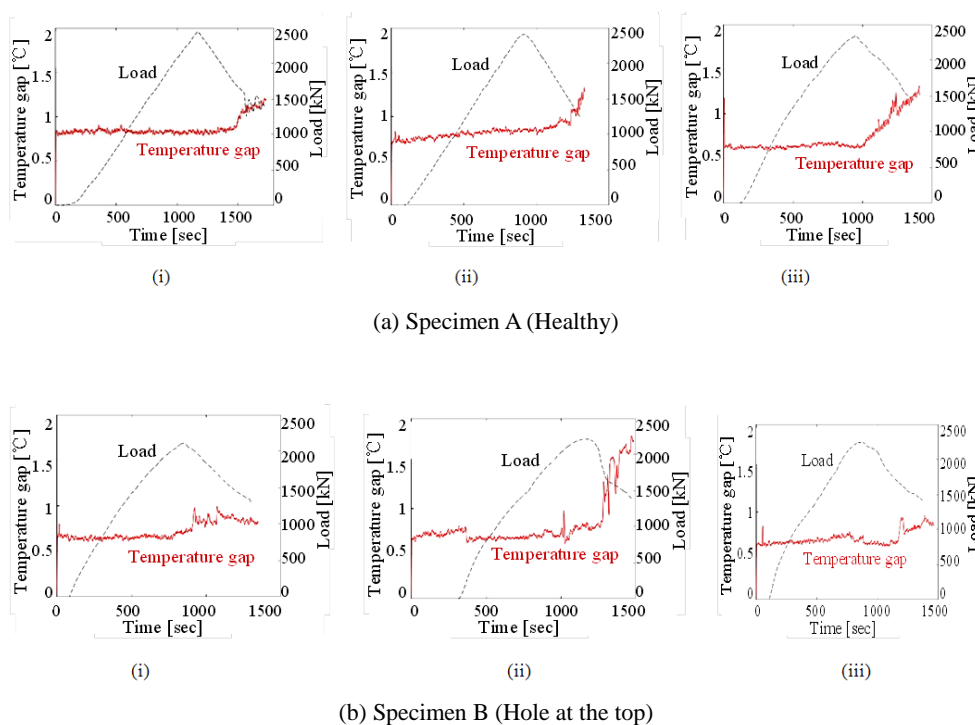
Comparison of measurements of time changes in surface temperatures for different surface conditions of healthy specimen A from Figure 6(a) shows the following: (i) the temperature difference without gelled resin is approximately 0.3 °C; (ii) the temperature difference with gelled resin (without mixture) is approximately 0.3 °C. The results were temperature differences of approximately 0.5 °C and (iii) approximately 0.7 °C, respectively, for gel-like resin containing 5% aluminum. Comparison of the time changes in the surface temperature of specimen B with defects created on the upper part of the specimen shown in Figure 6(b) shows the following: (i) about 0.3 °C difference with no gel resin and (ii) with gel resin (no mixture). The temperature differences were approximately 1.0 °C for (iii) gel-like resin containing 5% aluminum, and approximately 0.3 °C for (iii) gel-like resin containing 5% aluminum. Comparison of the time changes in the surface temperature of specimen C with defects created at the bottom of the specimen shown in Figure 6(c) shows the following: (i) the case without gel-like resin shows about 0.8 °C difference; (ii) the gel-like resin (without mixture) difference in temperature was approximately 0.5 °C; and (iii) the temperature difference was approximately 1.0 °C for the gel-like resin containing 5% aluminum.

For test specimens A and C, a greater temperature difference was maintained when gel resin was applied than when it was not applied. Additionally, a large temperature difference was observed in specimens that contained aluminum powder

compared to specimens that did not contain aluminum powder. However, specimen B coated with gel-like resin containing 5% aluminum in Figure 6(b) (iii) had the same temperature difference as the case without gel-like resin coated in Figure 7(b) (i). The result is 0.7 °C lower than that found for gel-like resin (without aluminum powder). The temperature difference in the gel-like resin containing 5% aluminum in specimen B did not become large, probably because the crack width was less than in other results. Although cracks propagated in three directions from the hole created as a defective part, each crack was small because the cracks were dispersed.

4.3. Knowledge Obtained from This Experiment

The gel-like resin coating prevented the specimen surfaces from blistering, suggesting that it is effective in preventing destruction. Even under these conditions, it was possible to inhibit fracture propagation and to inhibit the crack depth and size in areas where gel-like resin was applied. The gel-like resin application has been demonstrated as effective: it is probably effective for preventing collapses inside tunnels and for preventing falling objects from deteriorating over time, such as on concrete piers. Particularly when a gel-like resin is applied to the concrete surface, instant measurement using an infrared camera can be done when lifting or cracking occurs because of deterioration. The method is also expected to be effective as a preventive measure for halting crack propagation. Various tests must be done to enhance the reproducibility and reliability of these results. For example, crack depth must be measured using two infrared thermal imaging cameras.



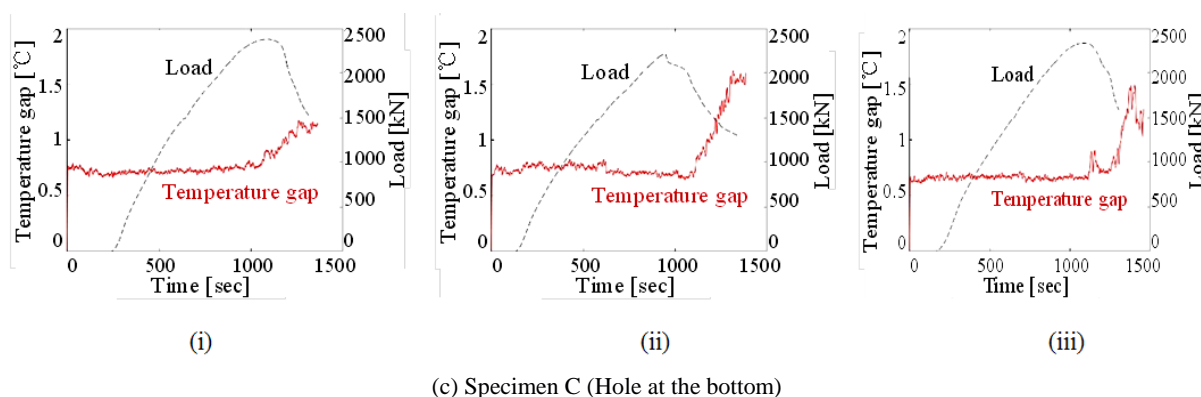


Figure 6. Comparison of infrared images with and without resin coating of specimens A, B, and C for crack temperature and surface temperature.

5. Conclusion

This measurement technology provided the following findings.

- (1) To improve the resolution of long-wavelength infrared thermal images, the temperature difference from the outside air must be increased. The compressive effect of this gel resin sensor applied to the surface of the specimen can maintain large differences in radiant heat from the fractured area, even when the specimen's internal temperature is lower than the outside temperature, thereby providing clear infrared thermal images of the damaged area. Theoretically, the difference between the temperature at the measurement point and the outside temperature should be about 5 °C, but gel-like resin mixed with aluminum powder can support measurements with temperature differences of 1 °C or less.
- (2) When a reinforced concrete specimen is subjected to compressive loading from the vertical direction, shear failure occurs first. Then the central part expands from side to side. Particularly with destructive testing of test specimens with holes assuming defects, observing the crack appearance around a hole in a chronological sequence has been impossible to using a conventional visible light camera. However, an infrared thermal imaging camera can visualize aspects that are invisible to the naked eye.
- (3) The gel resin coated sensor improves thermal image acquisition performance during passive measurement. Compared to 3–5 μm wavelength infrared cameras used for infrared thermal image measurements, 8–14 μm wavelength infrared cameras are cheaper and have a wider range. The cameras can obtain results suitable for measuring “peeling” and “lifting”. This method is also expected to be useful as a construction method to prevent shearing and peeling progression during destruction, and to prevent falling debris and collapse ac-

cidents.

- (4) To prevent cracks in structures and corrosion of reinforcing bars, rainwater must be prevented from entering. The applied resin is thought to prevent rainwater ingress and subsequent metal corrosion and deterioration.
- (5) Infrared thermal imaging showed the surface coating effect of this resin to be effective at suppressing swelling and surface peeling because of deformation of the reinforced concrete column during loading.

Abbreviations

FEM	Finite Element Method
LDV	Laser Doppler Velocimeter
MRIR	Medium Wave Infrared Detector
LWIR	Long Wave Infrared Detector

Acknowledgments

We thank Dr. Hiroshi Fukui, Senior Research Scientist of Dow Toray Co. Ltd. and Mr. Takashi Harasaki of Commercial Manager of Dow Toray Co. Ltd. for providing test materials and expert advice about resins. In other hand, This research was partially supported by JSPS KAKENHI Grant No. 20H00290, for which we express our appreciation.

Author Contributions

Nobuhiro Shimoi: Writing – original draft
Yu Yamauch: Writing – original draft
Kazuhisa Nakasho: Writing – original draft

Conflicts of Interest

The authors declare no conflicts of interest.

References

- [1] Ministry of Land, Infrastructure, & Transport. Infrastructure maintenance information. Available from https://www.mlit.go.jp/sogoseisaku/maintenance/02research/02_01_01.html (accessed on 10 October, 2020). (in Japanese).
- [2] Nobuhiro Shimoi, Yu Yamauch, Kazuhisa Nakasho, "Preventive Work and Health Monitoring for Technology by Cracks of Concrete Surface Using Coating Type Resin Sensor", International Journal of Sensors and Sensor Networks. Vol. 11, No. 1, 2023, pp. 1-10. <https://doi.org/10.11648/j.ijssn.20231101.11>
- [3] Matsuoka, H., Hirose, Y., Kurahashi, T., Murakami, Y., Toyama, S., Ikeda, H., Iyama, T. & Ihara, I. (2018) Application of a joint variable method for high accurate numerical evaluation of defect based on hammering test. Journal of the Society of Materials Science, Vol. 67, No. 9, pp. 869-876. (in Japanese). <https://doi.org/10.2472/jsms.67.876>
- [4] Shimoi, N., Nishida, T., Obata, A., Nakasho, K., Madokoro, H. & Cuadra, C. (2016) Comparison of displacement measurements in exposed type column base using piezoelectric dynamic sensors and static sensors. American Journal of Remote Sensing, Vol. 4, No. 5, pp. 23-32. (in Japanese). <https://doi.org/10.11648/j.ajrs.20160405.11>
- [5] Ueda, H., Ushijima, S. & Shyutto, K. (2007) Properties and deterioration prediction of acid attacked concrete. Japan Society of Civil Engineers, Vol. 63 No. 1, pp. 27-41 (in Japanese). <https://doi.org/10.2208/jsceje.63.27>
- [6] Tamai, H. (2003) Elasto Plastic Analysis Method for frame with exposed-type column base considering influence of variable axial force. Journal of Structural and Construction Engineering, Vol. 68, No. 571, pp. 127-135. (in Japanese). https://doi.org/10.3130/aijs.68.127_3
- [7] Miyashita, T., Ishii, H., Fujino, Y., Shoji, T. & Seki, M. (2007) Understanding of high-speed train induced local vibration of a railway steel bridge using laser measurement and its effect by train speed. Japan Society of Civil Engineering A, Vol. 63, No. 2, pp. 277-296 (in Japanese). <https://doi.org/10.2208/jsceja.63.277>
- [8] Michimura, K. (2008) Deterioration diagnosis technology by infrared method. Material Life Society, Vol. 20, No. 1, pp. 21-26 (in Japanese).
- [9] Hayashi, H., Hashimoto, K. & Akashi, Y. (2013) Improving detection accuracy of concrete damage by infrared thermography. Japan Concrete Institute, Vol. 35, No. 1, pp. 1813-1818 (in Japanese). https://data.jci-net.or.jp/data_pdf/35/035-01-1298
- [10] Shimizu, K. (1987) The latest technology for far-infrared use. Industrial Technology Association, pp. 6-24 (in Japanese).
- [11] Shimoi, N. (2001) The technology of personal mine detecting for humanitarian demining. SICE, Vol. 37, No. 6, pp. 577-583 (in Japanese). <https://doi.org/10.9746/sicetr1965.37.577>
- [12] Ono, K. (2003) Study on technology for extending the life of existing structures, New urban society technology fusion research. The Second New Urban Social Technology Seminar, pp. 11-23 (in Japanese).
- [13] Nakamura, M. (2002) Health monitoring of building structures. Society of Instrument and Control Engineers, Vol. 41, No. 11, pp. 819-824 (in Japanese). <https://doi.org/10.11499/sicej11962.41.819>
- [14] Kumagai, K., Nakamura, H. & Kobayashi, H. (1999) Computer aided nondestructive evaluation method of welding residual stresses by removing reinforcement of weld. Transactions of the Japan Society of Mechanical Engineers, Series A, Vol. 65, No. 629, pp. 133-140 (in Japanese). <https://doi.org/10.1299/kikaia.65.133>
- [15] Hashizume, K., Hashimoto K., Matsuda Y. (2017) Inspection of bridges, tunnels, and pavements using visible light, infrared light, etc. Journal of Automotive Engineering (Measurement and Control), Vol. 56, No. 11, pp. 884-887.
- [16] Malgague, X. (2002) Introduction to NDT by active infrared thermography. Materials Evaluation, pp. 1-22. (in Japanese)
- [17] Xu, J., Wang, H., Duan, Y., He, Chen, S. & Zhang, Z. (2020) Terahertz imaging vibro-thermography for impact response in carbon fiber reinforced plastics. Infrared Physics & Technology, Vol. 109, pp. 1-7. <https://doi.org/10.1016/j.infrared.2020.103413>